Modeling the additive effects of Pb(II) and Cu(II) on the competitive attenuation of As(V) through solid precipitation *versus* adsorption to goethite

Katherine Vaca-Escobar[1], Mario Villalobos[2,*]

[1] Posgrado en Ciencias de la Tierra, Instituto de Geología, UNAM, Ciudad Universitaria, Coyoacán, México DF 04510, México.
[2] Departamento de Geoquímica, Instituto de Geología, UNAM, Ciudad Universitaria, Coyoacán, México DF 04510, México.

[*] mar.villa@stanfordalumni.org

Abstract

Mine-related activities cause widespread contamination of aqueous environments with high concentrations of arsenic and accompanying heavy metals. The natural attenuation of As(V) in soils and groundwater under oxic conditions occurs mainly through sorption processes to iron and aluminum (hydr)oxides; as well as through the formation of highly insoluble heavy metal(II) arsenates.

In the present investigation we used thermodynamic modeling to predict the environmental geochemical behavior of As(V) in the presence of Pb(II), Cu(II) and goethite, in an effort to approach the complexity of multi-component real contaminated scenarios. The key to this modeling was the coupling of a highly robust Surface Complexation Model of As(V) adsorption to goethite, which uses combined tenets of the Triple-Layer and CD-MUSIC models, together with appropriate metal(II) arsenate solid formation constants as well as those of all chemical equilibria taking place in the aqueous phase. Mixed-metal arsenates were predicted to form and increase the predominance region of the precipitation reactions for a highly surface-reactive goethite, at the expense of the adsorption mechanism, but the model yielded no aqueous As(V) released at any condition investigated.

Keywords: Adsorption, precipitation, arsenate, goethite, lead, copper, Surface Complexation Model, Triple-Layer Model, CD-MUSIC Model.

Resumen

Las actividades relacionadas con la minería provocan contaminación extendida de ambientes acuosos conjuntamente de arsénico y metales pesados. La atenuación natural de As(V) en suelos y acuíferos en condiciones óxicas ocurre principalmente a través de procesos de adsorción a (hidr)óxidos de hierro y aluminio; así como a través de la formación de arseniatos de metales(II) pesados altamente insolubles.

En esta investigación utilizamos modelación termodinámica para predecir el comportamiento geoquímico ambiental del As(V) en presencia de Pb(II), Cu(II) y goetita, tratando de aproximarnos a la complejidad de escenarios multicomponentes de contaminación real. La clave de esta modelación fue el acoplamiento de un modelo de complejación superficial altamente robusto de adsorción de As(V) en goetita, el cual utiliza postulados combinados de los modelos de Triple Capa y CD-MUSIC, junto con constantes apropiadas de formación de arseniatos de metales divalentes sólidos y de todos los equilibrios químicos que ocurren en la fase acuosa. Se predice la formación de arseniatos metálicos mixtos que aumentan la región de predominio de las reacciones de precipitación, a expensas del mecanismo de adsorción en goetitas de alta reactividad superficial, pero el modelo predice que no se libera As(V) acuoso en ninguna de las condiciones investigadas.

Palabras clave: Adsorción, precipitación, arseniato, goetita, plomo, cobre, Modelo de Complejación Superficial, Modelo de Triple Capa, Modelo CD-MUSIC.

1. Introduction

Arsenic is a metalloid constituent of more than 245 minerals, and is associated most frequently with other metals such as copper, gold, lead, and zinc in sulfidic ores (Cullen and Reimer, 1989; Oremland and Stolz, 2003; Shen *et al*., 2013). Many sources of arsenic contamination result from human activities like the disposal of industrial chemical wastes, including mine wastes, the smelting of arsenic-bearing minerals, the burning of fossil fuels and the application of arsenic compounds in many products, especially in the past few hundred years (Garelick *et al*., 2008; Chang *et al*., 2009; Mirza *et al*., 2014). For example, arsenic concentrations measured in soils near a lead smelter were in average 2 g kg^{-1}, near a copper smelter 0.55 g kg^{-1}, and near a gold smelter from 0.5 to 9.3 g kg^{-1} (Bissen and Frimmel, 2003).

The reduction of arsenic levels in contaminated drinking water and soils is one of the priority environmental challenges worldwide (Thirunavkukkarasu *et al*., 2002). In Mexico, arsenic contamination problems in water and soils have been reported in the following regions: Villa La Paz, San Luis Potosí (Gamiño-Gutiérrez *et al*., 2013); Matehuala, San Luis Potosí (Martínez-Villegas *et al*., 2013); Comarca Lagunera in NW Mexico (Ordáz *et al*., 2013); Zimapán, Hidalgo (Romero *et al*., 2008); Guanajuato (Arroyo *et al*., 2013); and Zacatecas and Guadalupe, Zacatecas (Mireles *et al*., 2012). To reduce arsenic contamination, it is of utmost importance to understand all aspects of arsenic environmental geochemistry, which in turn will provide useful information to optimize treatment and remediation schemes for contaminated environments.

The reactivity of Arsenate [As(V)] with individual soil minerals determines the general mobility of arsenic in soils. As(V) is the predominant inorganic species of arsenic under oxidizing soil conditions (Goldberg, 2011; Camacho *et al*., 2011), and is retained in soils by adsorption processes (Goldberg and Glaubig, 1988; Smith and Naidu, 2009). Important minerals that control the As(V) adsorption capacity of soils include Fe and Al oxides, such as goethite, ferrihydrite, gibbsite, etc. (Violante *et al*., 2010; Smedley and Kinniburgh, 2013). However, there is evidence that in situations where the metal contents that accompany As(V) are high (as in smelting, mining and metallurgical wastes), formation of (highly insoluble) heavy metal arsenates occurs, such as duftite, mimetite, hydroxymimetite and bayldonite, making precipitation the predominant immobilization mechanism over the adsorption process (Gutierrez-Ruiz *et al*., 2005; Villalobos *et al*., 2010; Drahota and Filippi, 2009; Vaca-Escobar *et al*., 2012). For example, Villalobos *et al*. (2010) reported various As-contaminated soils with pH values between 4.5 and 10.2, As/Fe molar ratios of 0.03 – 2.5, As/Pb molar ratios of 0.53 – 300, and As/Cu molar ratios of 0.44 – 32, in which the presence of mixed heavy metal arsenates was identified.

In the present research, we use thermodynamic modeling to investigate the environmental geochemical conditions of arsenate mobility in aqueous environments, focusing on the competition between formation of Pb and Cu arsenates and adsorption mechanisms to an Fe oxide. We chose goethite because it is thermodynamically one of the most stable iron oxides in the environment (Schwertmann and Cornell, 2007), and therefore it is well characterized and the subject of many studies on surface complexation modeling (Hayes *et al*., 1991; Mathur and Dzombak, 2006). We build from our previous research with Pb(II)-only arsenate/goethite systems (Vaca-Escobar *et al*., 2012), in a "bottom-up" approach to progressively describe more complex systems in a quantitative manner, particularly those with various heavy metals present simultaneously. In this previous work we found that As(V) adsorption is favored at low As/Fe molar ratios (less than 0.021) or high As/Pb molar ratios (above 0.667), but also with highly reactive goethites of large particle sizes. In opposite conditions, Pb(II) precipitation becomes the more competitive immobilizing mechanism (Vaca-Escobar *et al*., 2012).

The main question asked here is whether the simultaneous presence of Cu(II) with Pb(II) promotes a higher predominance of precipitated metal arsenates *versus* As(V) adsorption to goethite, and to what extent this occurs. Also, in conditions that favor precipitation, how prevalent are the mixed Pb(II)-Cu(II) arsenates in comparison with the single Pb(II) or Cu(II) arsenates.

2. Materials and methods

2.1. Thermodynamic modeling

The arsenic species distribution was calculated by thermodynamic modeling using the Visual Minteq geochemical equilibrium and speciation interface, version 3.0 (Gustafsson, 2010). This program was updated with surface complexation constants for goethite reported by Salazar-Camacho and Villalobos (2010). These authors used combined tenets of the Triple-Layer and CD-MUSIC surface complexation models (SCMs) to describe in a unified manner the adsorption behavior of goethite, irrespective of its specific surface area (SSA), by defining the adsorption reactions per type of reactive site on the goethite surface. The two goethites for which the unified model has been calibrated have SSAs of 50 m^2 g^{-1} (GOE50) and a 94 m^2 g^{-1} (GOE94) (Salazar-Camacho and Villalobos, 2010). The latter corresponds to small ideal goethite crystals, and the former to larger particles that show higher reactivity per unit area.

Table 1 lists all surface complexation constants used, including their expressions and corresponding formation reactions. Binary adsorption data for the unified goethite model were available for As(V) and Pb(II) (Salazar-Camacho and Villalobos, 2010), but not for Cu(II). Pb(II) shows a higher binding affinity for goethite (and other

Table 1. Surface complexation reactions uploaded in Visual Minteq with formation constants described per type of surface site (Vaca-Escobar *et al.*, 2012; Villalobos *et al.*, 2009).

REACTIONS [a]	Log K [b]		
Acid-base [c]:	*FeOH*	*Fe$_2$OH*	*Fe$_3$OH*
$SOH + H^+ \rightleftharpoons SOH_2^+$	6.8	nr	7.66
$SOH \rightleftharpoons SO^- + H^+$	-10.8	nr	-11.66
Electrolytes complexation (outer-sphere):			
$SOH + H^+ + NO_3^- \rightleftharpoons SOH_2^+ \cdots NO_3^-$	8.02	nr	9.025
$SOH + Na^+ \rightleftharpoons SO^- \cdots Na^+ + H^+$	-9.43	nr	-11.095
Inner-sphere complexation:			
$SOH + Pb^{2+} \rightleftharpoons SOPb^+ + H^+$	0.64	nr	nr
$FeOH + SOH + H^+ + AsO_4^{3-} \rightleftharpoons FeO^{-0.7}AsO_3^{-1.3\cdots} HSO + H_2O$	21.6	18.75	nr
$FeOH + SOH + 2H^+ + AsO_4^{3-} \rightleftharpoons FeO^{-0.7}AsO_3^{-1.3\cdots} HOS + H_2O$	nr	19.6	nr
$SOH + H^+ + CO_3^{2-} \rightleftharpoons SO^{-0.2}CO_2^{-0.8} + H_2O$	13.55	13.32	nr
Outer-sphere complexation:			
$SOH + Pb^{2+} + H_2O \rightleftharpoons SO^- \cdots PbOH^+ + 2H^+$	-10.1	-8.6	nr

[a] SOH can be FeOH, Fe$_2$OH or Fe$_3$OH groups. As(V) surface complexation constants were taken from (Salazar-Camacho and Villalobos, 2010), and those for Pb(II) from (Villalobos *et al.*, 2009).

[b] nr = non-reactive group.

[c] The log of acidity constants used was established through a ΔpKa of 4 around each pH of PZNPC for each site type, which were 8.8 and 9.66, for FeOH and Fe$_3$OH groups, respectively.

minerals) than Cu(II) (Christophi and Axe, 2000). Therefore, we hypothesized that As(V) (Kingston *et al.*, 1972) and Pb(II) (Kooner, 1993) adsorption are sufficiently stronger than Cu(II) adsorption to goethite, and that the exclusion of the latter would not affect the modeling results. To test this hypothesis, we modeled the Pb(II)/As(V)/goethite system in the presence and absence of the binary Pb(II) adsorption reactions. We found no difference in the As(V) speciation results, but only in the case of the more surface reactive GOE50. Therefore, we decided to perform the modeling for the complete system including Cu(II) only with this GOE50, and for the moment to exclude GOE94 since we could not ensure that the absence of Cu(II) surface binding constants would affect the results for the latter.

To complete the SCM, in addition to the surface complexation constants, other input parameters are required. They include: the specific surface area (50m^2 g^{-1}); the surface site density (see below); two electrical capacitances (C$_1$ = 1.17 F m^{-2} and C$_2$ = 0.20 F m^{-2}); a fixed GOE50 solids concentration (0.2 g L^{-1}); ionic strength (I = 0.01 mol L^{-1} NaNO$_3$); and LogPCO$_2$ = -3.5. Computations were performed by varying the concentration of total As(V), essentially increasing the total As/Fe ratio.

The surface site density is dependent on the contribution of the specific exposed crystal faces of the goethite sample used. It is calculated from chromate adsorption maxima at pH 4. For the 50m^2 g^{-1} goethite they are: 6.86 sites nm^{-2} for ≡FeOH; 2.87 sites nm^{-2} for ≡Fe$_2$OH; and 1.12 sites

nm^{-2} for ≡Fe$_3$OH groups; with a face distribution of 37 % for {101} and 63 % for {010} (Salazar-Camacho and Villalobos, 2010).

The SCM was coupled to an aqueous and solid thermodynamic speciation model, for which the corresponding available formation constants of all species are listed in Table 2. The complete thermodynamic model applied was validated previously by wet chemical experimental results, which matched closely the model results for the As(V)/Pb(II)/goethite system (Vaca-Escobar *et al.*, 2012). Therefore, we are confident that the model employed represents well the behavior of the system when one additional component, *i.e.*, Cu(II), is added, so no additional experimental verification of the model results was performed.

For the As(V)/Pb(II)/Cu(II) system, two different ratios of total concentrations added were chosen (1/1/1 and 2/1/3) to represent those of the two main mixed-metal arsenates that form: duftite [PbCu(AsO$_4$)(OH)] and bayldonite [PbCu$_3$(AsO$_4$)$_2$(OH)$_2$].

3. Result

The first step was to determine the solid speciation expected as a function of pH in the absence of adsorption processes, in order to gain knowledge of the metal(II) solids expected to compete for As(V) binding with the goethite

Table 2. Solid and aqueous species formation constants from their components, used in the thermodynamic model (Taken from Visual Minteq Database).

Mineral Name	Chemical Formula	Log K_f
SOLID SPECIES		
Hydroxymimetite	$Pb_5(AsO_4)_3OH$	62.115 [a]
Plumbonacrite	$Pb_{10}(OH)_6O(CO_3)_6$	8.76
Schultenite	$PbHAsO_4$	23.969 [a]
Hydrocerrusite	$Pb_3(OH)_2O(CO_3)_2$	18.77
Cerrusite	$PbCO_3$	13.13
Shannonite	Pb_2OCO_3	0.558
Massicot	PbO	-12.894
Litharge	PbO	-12.694
Natron	$Na_2CO_3.10H_2O$	1.311
Thermonatrite	$Na_2CO_3.H_2O$	-0.637
Azurite	$Cu_3(CO_3)_2(OH)_2$	16.906
Malachite	$Cu_2(CO_3)(OH)_2$	5.306
Tenorite (c)	CuO	-7.644
Tenorite (am)	CuO	-8.49
Bayldonite	$PbCu_3(AsO_4)_2(OH)_2$	37.05
Duftite	$PbCu(AsO_4)(OH)$	20.512
	$CuCO_3$	11.5
	$Cu_3(AsO_4)_2.2H_2O$	35.119
	$Cu(OH)_2$	-8.674
	$Pb_3O_2CO_3$	-11.02
	PbO	-8.15
	$Pb_2O(OH)_2$	-26.188
	$Pb(OH)_2$	-8.15
	$PbO.0.3H_2O$	-12.98
	As_2O_5	34.694
AQUEOUS SPECIES		
	$Cu_2(OH)_2^{2+}$	-10.494
	$Cu(CO_3)_2^{2-}$	10.2
	$Cu(NO_3)_2$	-0.4
	$Cu(OH)_2$	-16.23
	$Cu(OH)_3^-$	-26.64
	$Cu(OH)_4^{2-}$	-39.73
	Cu_2OH^{3+}	-6.71
	$Cu_3(OH)_4^{2+}$	-20.788
	$CuCO_3$	6.77
	$CuHCO_3^+$	12.129
	$CuNO_3^+$	0.5
	$CuOH^+$	-7.497
	$NaNO_3$	-0.55
	$NaOH$	-13.897
	OH^-	-13.997
	$HAsO_4^{2-}$	11.6
	$H_2AsO_4^-$	18.35
	H_3AsO_4	20.6
	$PbH_2AsO_4^+$	19.736 [a]
	$PbHAsO_4$	14.038 [a]
	$Pb(OH)_2$	-17.897
	$Pb(NO_3)_2$	1.4
	$PbNO_3^+$	1.17
	$PbOH^+$	-7.597
	$Pb_4(OH)_4^{4+}$	-19.988
	$Pb_2(OH)^{3+}$	-6.397
	$Pb(OH)_3^-$	-28.091
	$Pb(OH)_4^{2-}$	-39.699
	$Pb_3(OH)_4^{2+}$	-23.888
	H_2CO_3	16.681
	HCO_3^-	10.329
	$NaHCO_3$	10.079
	$PbHCO_3^+$	13.2
	$NaCO_3^-$	1.27
	$PbCO_3$	6.478
	$Pb(CO_3)_2^{2-}$	9.938

[a] Log Kf taken from Villalobos *et al*., 2010 and included in Visual Minteq Database.

surface (Figure 1). Table 3 summarizes the results by reporting the expected solids and their stability pH range at the different As(V)-Cu(II)-Pb(II) molar ratios studied.

After this, the complete model that includes adsorption onto goethite (GOE50) was applied, and the sum of three main types of As(V) species predicted – adsorbed, precipitated and dissolved – were plotted as percentage of the total As(V) applied. This was done as a function of the molar As/Fe ratio, to determine the species contributions as As(V) increased relative to goethite (Figures 2 and 3).

3.1. Simple As(V)-Pb(II) systems

The As(V)/Pb(II) system was investigated previously and the mineral hydroxymimetite $[Pb_5(AsO_4)_3OH]$ was identified as the main solid forming in a pH range of 5 to 9 (Vaca-Escobar *et al*., 2012).

When adsorption processes to GOE50 were included in the model, this retention mechanism controlled As(V) speciation, and precipitation of hydroxymimetite did not occur until all surface sites were saturated, as As/Fe was increased. This was in stark contrast to the behavior shown by GOE94, in which precipitation of hydroxymimetite occurred considerably before surface site saturation with As(V) was attained, and quickly became the predominant mechanism as As/Fe was further increased (Vaca-Escobar *et al*., 2012).

3.2. Simple As(V)-Cu(II) systems

A Cu(II) arsenate is predicted to precipitate in a very narrow pH range around 6, which is the pH of minimal As(V) solubility for As/Cu molar ratios of 1 (Figure 1a) and 2/3 (Figure 1b). Therefore, pH 6 was one of the values chosen for further investigations in the complete system.

In the presence of goethite, adsorption of As(V) was not disrupted by the presence of Cu(II) (Figure 2). Even after surface site saturation is reached as As/Fe is increased, before the onset of the Cu(II) arsenate precipitation, dissolved As(V) reached values above 40 % at the maxima for both As/Cu ratios investigated at pH 6. At an As(V)/Cu(II) molar ratio of 1 (Figure 2a) the dissolved species contribution stabilized at around 30 %. At the lower As(V)/Cu(II) molar ratio (2/3) the dissolved species decreased to less than 10 % at high As(V)/Fe(III) molar ratios (Figure 2b). Thus, precipitation of the arsenate became highly predominant in this latter system. Therefore, in comparison with the As(V)-Pb(II) systems, the As(V)-Cu(II) systems are predicted to be much less efficient in removing aqueous As(V).

3.3. As(V)-Pb(II)-Cu(II) systems

In the As(V) system where both metals are present a more complex precipitation behavior was observed (Figures 1c and d), in which several solids may coexist over wide
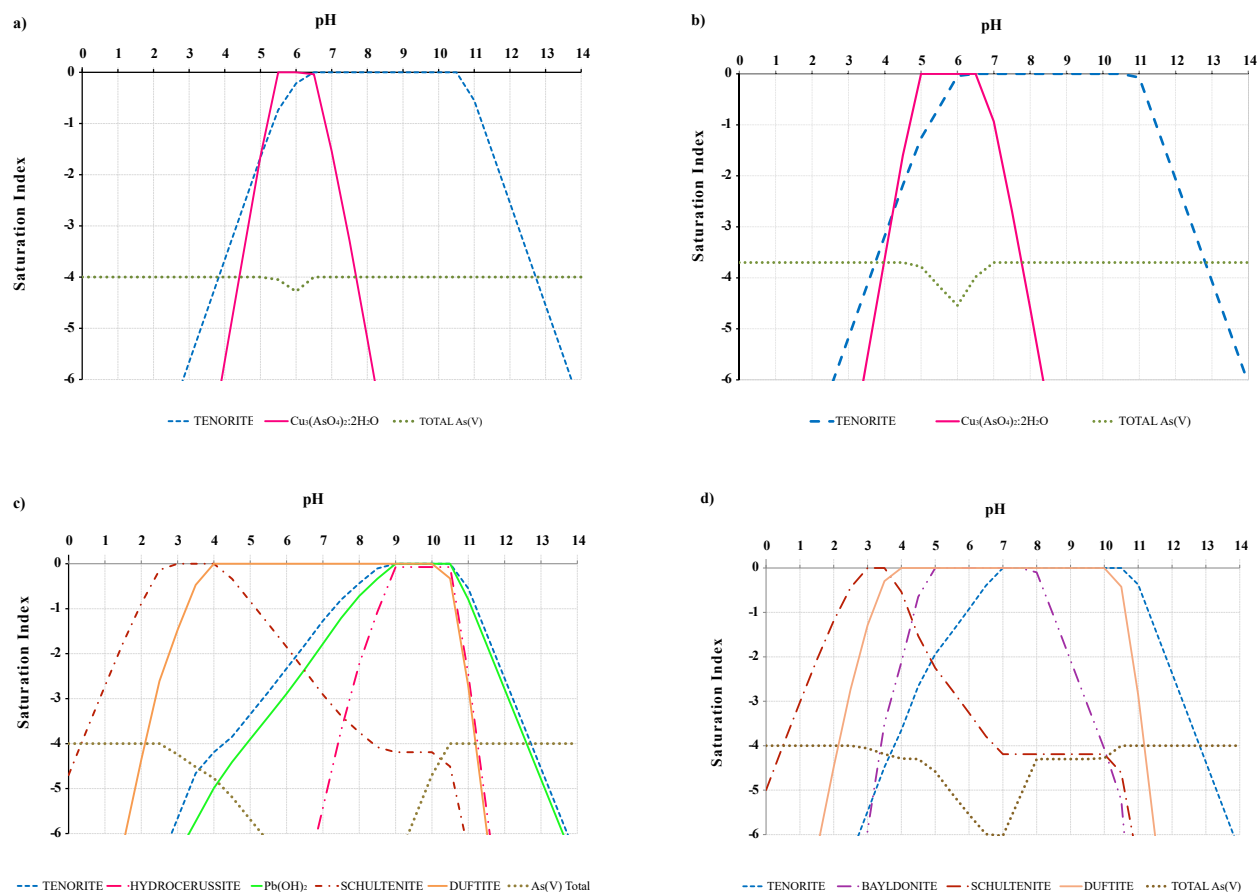
Figure 1. Saturation indices of As-Cu-Pb solids in the absence of goethite, for a system composed of a) $[AsO_4^{3-}] = 1 \times 10^{-4}$ M, $[Cu^{2+}] = 1 \times 10^{-4}$ M (As/Cu = 1/1); b) $[AsO_4^{3-}] = 2 \times 10^{-4}$ M, $[Cu^{2+}] = 3 \times 10^{-4}$ M (As/Cu = 2/3); c) $[AsO_4^{3-}] = 1 \times 10^{-4}$ M, $[Cu^{2+}] = 1 \times 10^{-4}$ M, $[Pb^{2+}] = 1 \times 10^{-4}$ M (As/Pb/Cu = 1/1/1); and d) $[AsO_4^{3-}] = 2 \times 10^{-4}$ M, $[Cu^{2+}] = 3 \times 10^{-4}$ M, $[Pb^{2+}] = 1 \times 10^{-4}$ M (As/Pb/Cu = 2/1/3). All systems have I = 0.01 M NaNO$_3$. Chemical formulas of solid minerals shown are listed in Table 2.

Table 3. pH range in which there are solid formations with respect to composition.

As/Pb/Cu molar ratio	Solid formed[a]	pH range
3/5/0[b]	Schultenite	3.5 – 5.0
	Hydroxymimetite	5.0 – 9.0
	PbO	8.0 – 10.5
1/1/0[a]	Schultenite	2.0 - 6.0
	Hydroxymimetite	5.0 – 9.5
	PbO	9.5 – 10.5
1/0/1	Cu$_3$(AsO$_4$)$_2$.2H$_2$O	5.5 – 6.5
	Tenorite	6.5 – 10.5
2/0/3	Cu$_3$(AsO$_4$)$_2$.2H$_2$O	5.0 – 6.5
	Tenorite	6.0 – 11.0
01/01/2001	Schultenite	3.0 – 4.0
	Duftite	4.0 – 10.0
	Tenorite	8.5 – 10.5
	Hydrocerussite	9.0 – 10.5
	PbO	9.0 – 10.5
02/01/2003	Schultenite	3.0 – 3.5
	Duftite	4.0 – 10.0
	Bayldonite	5.0 – 8.0
	Tenorite	7.0-10.5

[a] The corresponding chemical formulas are listed in Table 2.
[b] Molar ratios taken from Vaca-Escobar *et al.* (2012).

pH intervals (Table 3). For both As(V)/Pb(II)/Cu(II) molar ratios used in this research (1/1/1 and 2/1/3), pH 7 was chosen for investigating the system in the presence of goethite because at this value they showed the lowest As(V) solubility. At a 1/1/1 ratio the only solid predicted to form at pH 7 was duftite [PbCu(AsO$_4$)(OH)] (Figure 1c), while at the 2/1/3 ratio three simultaneous solids were predicted, two of them being mixed-metal arsenates: duftite [PbCu(AsO$_4$)(OH)], and bayldonite [PbCu$_3$(AsO$_4$)$_2$(OH)$_2$]. However, a much lower As(V) solubility was predicted in the former case ($10 - 7.6$ M — not shown in the scale of Figure 1c), in comparison to the latter ($10 - 6$ M — Figure 1d); as well as a wider pH range of insolubility.

In the systems that include adsorption to GOE50, the first important difference observed from those in the absence of Cu(II) is that the As/Fe region of predominance of the adsorption mechanism was diminished, on account of an increase in the corresponding region of arsenate precipitation. The As(V) insolubility behavior described above is well reflected here by showing a larger decrease in the adsorbed species distribution for the system with an As/Pb/Cu molar ratio of 1/1/1 (Figure 3a), and the
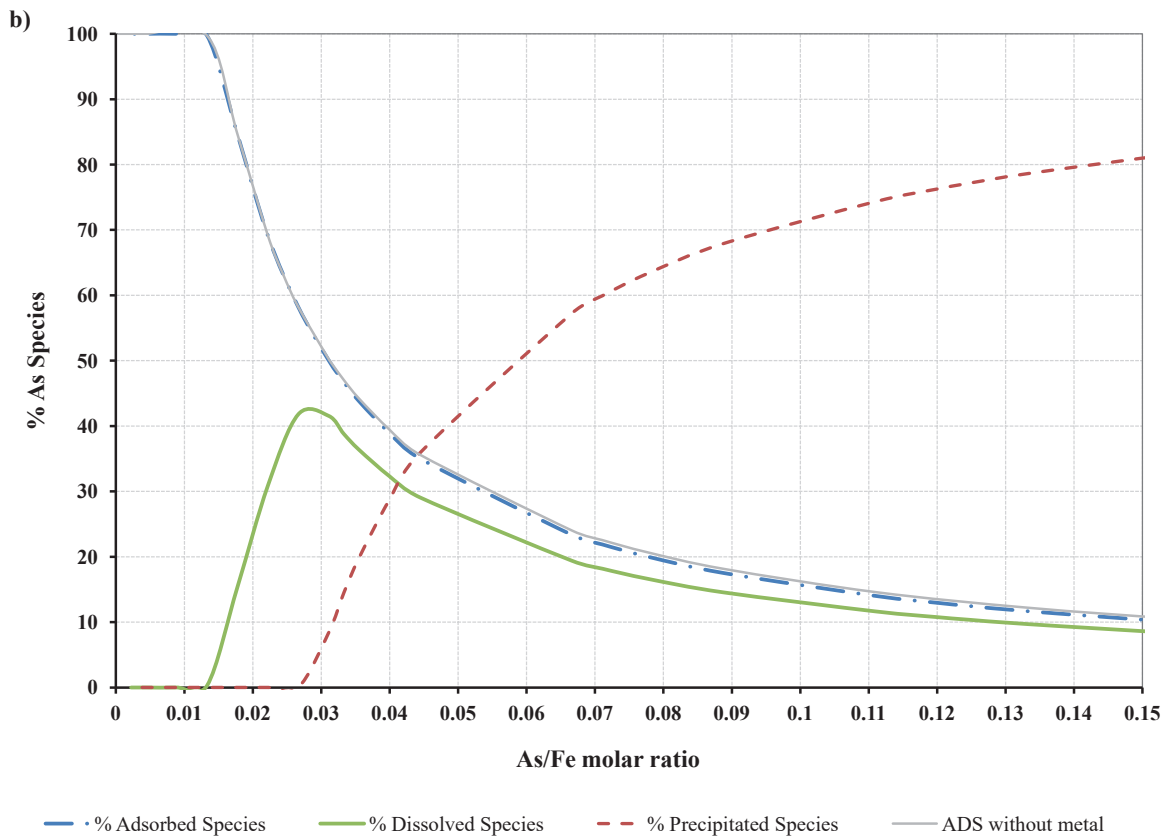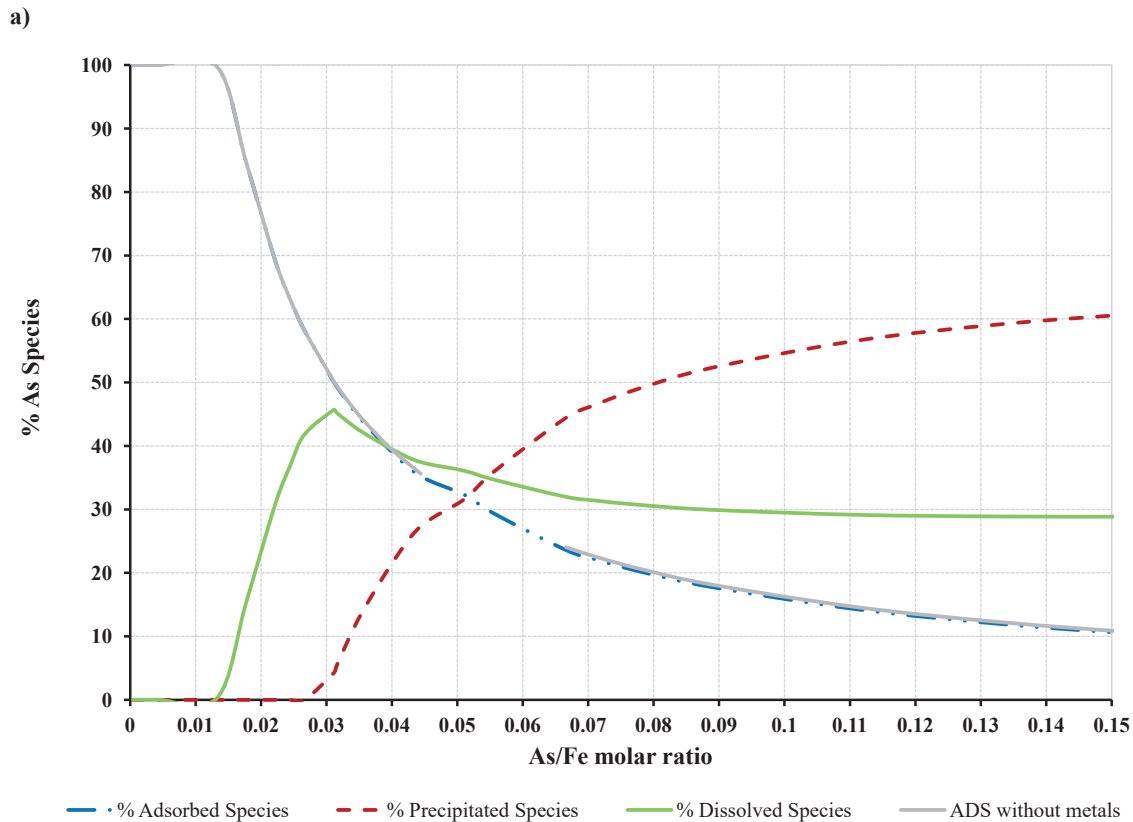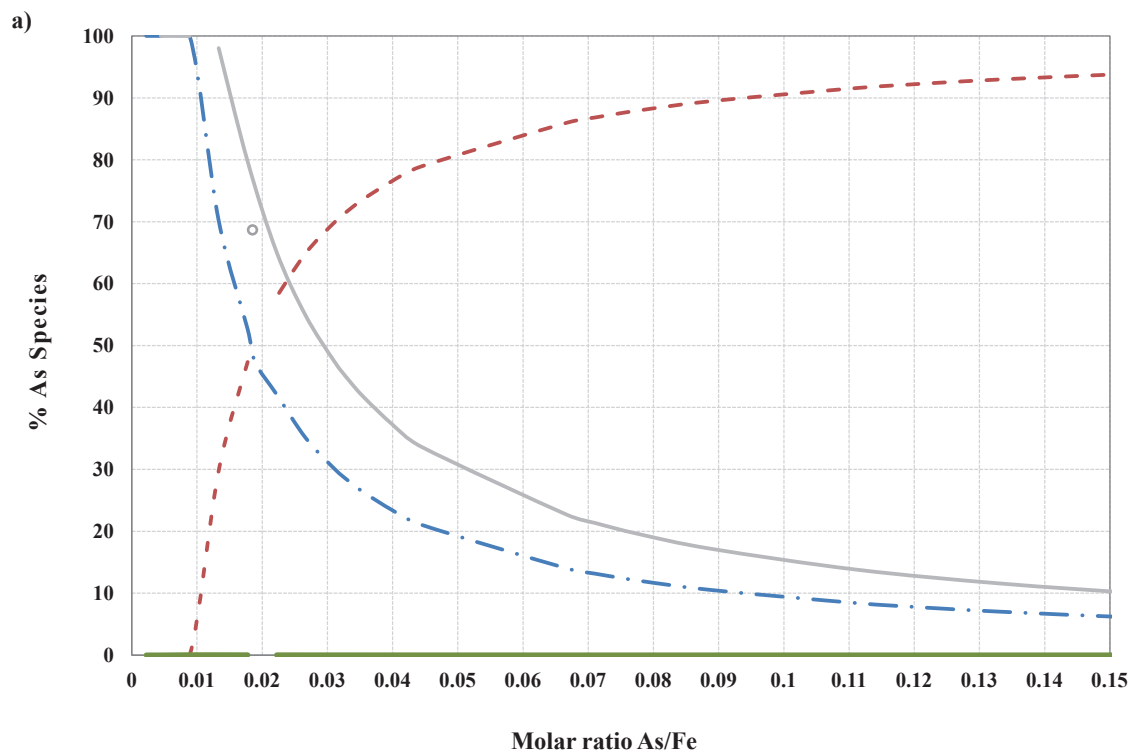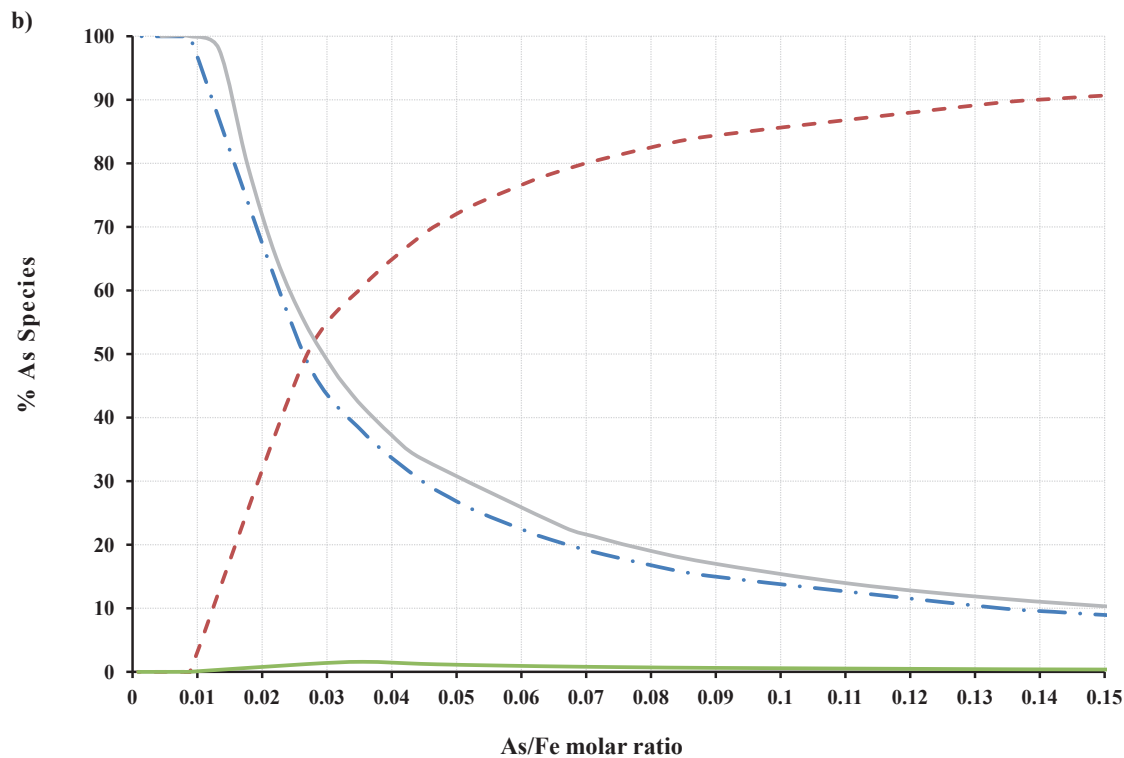
a)

b)

Figure 2. As(V) species distribution in the presence of Cu(II) and goethite (GOE50) at pH 6 and I = 0.01M NaNO$_3$ a) As/Cu molar ratio = 1, and b) As/Cu molar ratio = 2/3.

a)

b)

Figure 3 As(V) species distribution in the presence of Pb(II), Cu(II), and goethite (GOE50) at pH 7 and I = 0.01M NaNO3 a) As/Pb/Cu molar ratio = 1/1/1, and b) As/Pb/Cu molar ratio = 2/1/3.

corresponding increase in the precipitation of duftite, as compared to the system with a 2/1/3 ratio (Figure 3b). It is interesting to note that the onset of precipitation occurred at a very similar As/Fe ratio for both systems, but the former showed a considerably steeper precipitation curve, such that the crossing point where adsorption and precipitated species were equal appeared at a considerably lower As/Fe value (Figure 3a) than for the 2/1/3 system (Figure 3b) (0.019 for the 1/1/1 ratio and 0.027 for the 2/1/3 ratio).

In the 1/1/1 system at the As/Fe ratio of 0.01, at which site saturation occurs in the absence of metals, adsorption decreased to approximately 70 %; whereas in the 2/1/3 system the adsorption decrease was small (*ca.* to 90 %) at this As/Fe ratio, and the adsorption curve in general was close to the one in the absence of metals. Dissolved species did not appear in this system, because As(V) species were distributed exclusively between adsorbed and precipitated.

4. Discussion and conclusions

Thermodynamic modeling is a powerful tool for predicting the behavior of complex multi-component systems in which adsorption and solid mineral precipitation occur as potential attenuation processes. This is the case for As(V) in the presence of heavy metals (II) and goethite, for which accurate geochemical modeling is possible when a robust adsorption model is available. This research can be of great interest because we have not found other investigations that combine adsorption and precipitation processes in compounded thermodynamic modeling to predict As(V) behavior in soils, and to propose remediation methods.

Previously it was found that in the presence of Pb(II), As(V) may form very insoluble minerals before it saturates the goethite surface, but only for an ideal goethite of small particle sizes. For larger more surface-reactive goethites, the adsorption mechanism prevails, and precipitation does not occur until all surface sites are occupied, except in the presence of chloride because of mimetite formation, which is considerably more insoluble than other lead arsenates (Vaca-Escobar *et al.*, 2015).

In the present work we investigated the behavior of As(V) when a second metal component [Cu(II)] was added to the system, in an effort to approach the complexity of mine waste-contaminated environments. A considerable decrease in the adsorption of As(V) to a large goethite was found when the three components were added at a ratio of 1/1/1, in a similar fashion to the decrease observed in the presence of Cl⁻ and in the absence of Cu(II), due to formation of the extremely insoluble mimetite mineral (Vaca-Escobar *et al.*, 2015). The adsorption decrease in the presence of Cu(II) was caused by the precipitation of a mixed-metal arsenate called duftite: $PbCu(AsO_4)(OH)$.

At an added ratio of 2/1/3 for As/Pb/Cu, corresponding to another mixed-metal arsenate, bayldonite $[PbCu_3(AsO_4)_2(OH)_2]$, a much lower effect on the adsorption of As(V) to goethite was observed, despite the fact that both mixed Pb(II)-Cu(II) minerals are predicted to precipitate simultaneously.

In the mixed-metal systems none of the existing single-metal arsenates were predicted to form at the two ratios investigated, and no aqueous As(V) appeared under any of the conditions investigated. In this manner, the interplay between adsorption and precipitation, whether one mechanism or the other prevails, allows for an efficient attenuation of As(V) in aqueous systems contaminated with As(V) and heavy metals Pb(II) and Cu(II).

Conversely, in the As(V)/Cu(II) system [*i.e.*, without Pb(II) added], the Cu(II) arsenate solubility was not low enough to affect the adsorption process, and in fact a considerable fraction of aqueous As(V) appeared beginning from an As/Fe ratio of *ca.* 0.02. Therefore, it seems advantageous from an environmental perspective that more than one metal(II) be present simultaneously with As(V) in a contamination scenario to ensure their immobilization, in which the formation of insoluble mixed-metal arsenates seems to be a predominant attenuation mechanism. Given that mixed metal arsenates have been detected in contaminated soils, and that in previous laboratory experiments less than 14 days were required to reach equilibrium for Pb(II) arsenate solid formation, we believe no major kinetic impediments exist for the formation of mixed metal arsenates in contaminated environments.

The results of this work are highly relevant for understanding the environmental geochemistry of As(V) in aqueous environments, such as soils, with high contents of heavy metals, and for the conceptual design of efficient remediation schemes of As-contaminated environments by controlled addition of other heavy metal wastes in systems with a high As/Fe molar ratio.

References

Arroyo, Y.R.R., Muñoz, A.H.S., Barrientos, E.Y., Huerta, I.R., Wrobel, K., Wrobel, K., 2013, Natural Decrease of Dissolved Arsenic in a Small Stream Receiving Drainages of Abandoned Silver Mines in Guanajuato, Mexico: Bulletin of environmental contamination and toxicology, 91, 539–544.

Bissen, M., Frimmel, F.H., 2003, Arsenic — a Review. Part I: Occurrence, Toxicity, Speciation, Mobility: Acta Hydrochimica et Hydrobiologica, 31, 9–18.

Camacho, L.M., Gutiérrez, M., Alarcón-Herrera, M.T., Villalba, M.d.L., Deng, S., 2011, Occurrence and treatment of arsenic in groundwater and soil in northern Mexico and southwestern USA: Chemosphere, 83, 211–225.

Chang, J.-S., Yoon, I.-H., Kim, K.-W., 2009, Heavy metal and arsenic accumulating fern species as potential ecological indicators in As-contaminated abandoned mines: Ecological Indicators, 9, 1275–1279.

Christophi, C.A., Axe, L., 2000, Competition of Cd, Cu, and Pb adsorption on goethite: Journal of Environmental Engineering, 126, 66–74.

Cullen, W.R., Reimer, K.J., 1989, Arsenic speciation in the environment: Chemical Reviews, 89, 713–764.

Drahota, P., Filippi, M., 2009, Secondary arsenic minerals in the environment: a review: Environment international, 35, 1243–1255.

Gamiño-Gutiérrez, S., González-Pérez, C.I., Gonsebatt, M., Monroy-Fernández, M., 2013, Arsenic and lead contamination in urban soils of Villa de la Paz (Mexico) affected by historical mine wastes and its effect on children's health studied by micronucleated exfoliated cells assay: Environmental Geochemistry and Health, 35, 37–51.

Garelick, H., Jones, H., Dybowska, A., Valsami-Jones, E., 2008, Arsenic Pollution Sources: Reviews of environmental contamination and toxicology, 197, 17–60.

Goldberg, S., 2011, Chemical Equilibrium and Reaction Modeling of Arsenic and Selenium in Soils, *in* Selim, M. (ed.), Dynamics and Bioavailability of Heavy Metals in the Rootzone, 65–92.

Goldberg, S., Glaubig, R., 1988, Anion sorption on a calcareous, montmorillonitic soil—arsenic: Soil Science Society of America Journal, 52, 1297–1300.

Gustafsson, J.P., 2010, Visual MINTEQ Ver. 3.0. A free equilibrium speciation model software: Stockholm, Sweden, updated on 2013-11-27, *available at* <http://vminteq.lwr.kth.se/>, *consulted* 2015-11.

Gutierrez-Ruiz, M., Villalobos, M., Romero, F., Fernandez-Lomelin, P., 2005, Natural attenuation of arsenic in semiarid soils contaminated by oxidized arsenic wastes, *in* Oday, P.A., Vlassopoulos, D., Meng, Z., Benning, L.G. (eds.), Advances in Arsenic Research: Integration of Experimental and Observational Studies and Implications for Mitigation: American Chemical Society, ACS Symposium Series, Book 915, 235–252.

Hayes, K.F., Redden, G., Ela, W., Leckie, J.O., 1991, Surface complexation models: an evaluation of model parameter estimation using FITEQL and oxide mineral titration data: Journal of Colloid and Interface Science, 142, 448–469.

Kingston, F., Posner, A., Quirk, J.T., 1972, Anion adsorption by goethite and gibbsite: Journal of Soil Science, 23, 177–192.

Kooner, Z.S., 1993, Comparative study of adsorption behavior of copper, lead, and zinc onto goethite in aqueous systems: Environmental Geology, 21, 242–250.

Martínez-Villegas, N., Briones-Gallardo, R., Ramos-Leal, J.A., Avalos-Borja, M., Castañón-Sandoval, A.D., Razo-Flores, E., Villalobos, M., 2013, Arsenic mobility controlled by solid calcium arsenates: A case study in Mexico showcasing a potentially widespread environmental problem: Environmental Pollution, 176, 114–122.

Mathur, S., Dzombak, D., 2006, Surface complexation modeling: goethite: Interface Science and Technology, 11, 443–468.

Mireles, F., Davila, J.I., Pinedo, J.L., Reyes, E., Speakman, R.J., Glascock, M.D., 2012, Assessing urban soil pollution in the cities of Zacatecas and Guadalupe, Mexico by instrumental neutron activation analysis: Microchemical Journal, 103, 158–164.

Mirza, N., Mahmood, Q., Maroof Shah, M., Pervez, A., Sultan, S., 2014, Plants as Useful Vectors to Reduce Environmental Toxic Arsenic Content: The Scientific World Journal, 921581, 11 p.

Ordáz, G.H., Castruita, M.A.S., Pico, L.C.Á.G., Nuncio, R.A.A., Hernández, M.F., Cervantes, G.G., 2013, Comportamiento del arsénico en suelos de la región lagunera de Coahuila, México: Terra Latinoamericana, 31, 295–303.

Oremland, R.S., Stolz, J.F., 2003, The Ecology of Arsenic: Science, 300, 939–944.

Romero, F.M., Villalobos, M., Aguirre, R., Gutierrez, M.E., 2008, Solid-phase control on lead bioaccessibility in smelter-impacted soils: Archives of Environmental Contamination and Toxicology, 55, 566–575.

Salazar-Camacho, C., Villalobos, M., 2010, Goethite surface reactivity: III. Unifying arsenate adsorption behavior through a variable crystal face - Site density model: Geochimica et Cosmochimica Acta, 74, 2257–2280.

Schwertmann, U., Cornell, R.M., 2007, The Iron Oxides, *in* Schwertmann, U., Cornell, R.M. (eds.), Iron Oxides in the Laboratory: Weinheim, Federal Republic of Germany, Wiley-VCH, 5–18.

Shen, S., Li, X.-F., Cullen, W.R., Weinfeld, M., Le, X.C., 2013, Arsenic Binding to Proteins: Chemical Reviews, 113, 7769–7792.

Smedley, P.L., Kinniburgh, D., 2013, Arsenic in Groundwater and the Environment, *in* Selinus, O. (ed.), Essentials of Medical Geology: Netherlands, Springer, 279–310.

Smith, E., Naidu, R., 2009, Chemistry of inorganic arsenic in soils: kinetics of arsenic adsorption–desorption: Environmental Geochemistry and Health, 31, 49–59.

Thirunavkukkarasu, O.S., Viraraghavan, T., Subramanian, K.S., Tanjore, S., 2002, Organic arsenic removal from drinking water: Urban Water, 4, 7.

Vaca-Escobar, K., Villalobos, M., Ceniceros-Gomez, A.E., 2012, Natural arsenic attenuation via metal arsenate precipitation in soils contaminated with metallurgical wastes: III. Adsorption versus precipitation in clean As(V)/goethite/Pb(II)/carbonate systems: Applied Geochemistry, 27, 2251–2259.

Vaca-Escobar, K., Villalobos, M., Pi-Puig, T., Zanella, R., 2015, Approaching the geochemical complexity of As(V)-contaminated systems through thermodynamic modeling: Chemical Geology, 40, 162–173.

Villalobos, M., Cheney, M.A., Alcaraz-Cienfuegos, J., 2009, Goethite surface reactivity: II. A microscopic site-density model that describes its surface area-normalized variability: Journal of Colloid and Interface Science, 336, 412–422.

Villalobos, M., Garcia-Payne, D.G., Lopez-Zepeda, J.L., Ceniceros-Gomez, A.E., Gutierrez-Ruiz, M.E., 2010, Natural Arsenic Attenuation via Metal Arsenate Precipitation in Soils Contaminated with Metallurgical Wastes: I. Wet Chemical and Thermodynamic Evidences: Aquatic Geochemistry, 16, 225–250.

Violante, A., Cozzolino, V., Perelomov, L., Caporale, A.G., Pigna, M., 2010, Mobility and bioavailability of heavy metals and metalloids in soil environments: Journal of Soil Science and Plant Nutrition, 10, 268–292.